

Three-cluster breakup in deuteron-deuteron collisions: single-scattering approximation

A. Deltuva

*Institute of Theoretical Physics and Astronomy, Vilnius University,
A. Goštauto St. 12, LT-01108 Vilnius, Lithuania*

A. C. Fonseca

Centro de Física Nuclear da Universidade de Lisboa, P-1649-003 Lisboa, Portugal

(Received August 4, 2021)

We present results for the three-cluster breakup in deuteron-deuteron collisions at 130 and 270 MeV deuteron beam energy. The breakup amplitude is calculated using the first term in the Neumann series expansion of the corresponding exact four-nucleon equations. In analogy with nucleon-deuteron breakup where an equivalent approximation is compared with exact calculations, we expect this single-scattering approximation to provide a rough estimation of three-body breakup observables in quasifree configurations. We predict the nucleon-deuteron and deuteron-deuteron three-cluster breakup cross sections to be of a comparable size and thereby question the reliability of the recent experimental data [A. Ramazani-Moghaddam-Arani, Ph.D. thesis, University of Groningen, 2009; A. Ramazani-Moghaddam-Arani *et al.*, EPJ Web of Conferences **3**, 04012 (2010)] that is smaller by about three orders of magnitude. We also show that an equivalent single-scattering approximation provides a reasonable description of deuteron-deuteron elastic scattering at forward scattering angles.

PACS numbers: 21.30.-x, 21.45.-v, 24.70.+s, 25.10.+s

I. INTRODUCTION

In the last 20 years experimentalists have provided precise data for deuteron (d) breakup in the collision with a proton (p) at energies up to pion production threshold. Their motivation has been to look for regions of three-body phase space where the results are sensitive to the nucleon-nucleon (NN) interaction and the need to include a three-nucleon (3N) force. Given that there are numerically exact 3N calculations that include a wide variety of NN force models, comparison between theoretical calculations and precise data sheds light on the quality of the NN interactions that have been proposed. Since all NN interactions are fitted to NN elastic scattering data with equivalent χ^2 precision, possible disagreements may reside in the off-shell nature of the chosen NN interaction or the need to add a 3N force. Unfortunately this quest has been, in a few isolated cases such as the nucleon-deuteron analyzing power puzzle [1] or the space-star anomaly [2–4], overshadowed by persistent discrepancies between data and theory that defy comprehension within the framework of non-relativistic quantum mechanics applied to three interacting nucleons alone.

Up to now very few breakup data exist involving four-nucleon reactions, though this system shows extra sensitivity to NN force models as some calculations have already demonstrated [5–7] for specific spin observables and cross sections for elastic, charge exchange and transfer reactions. Nevertheless exact numerical four-nucleon calculations for breakup amplitudes are still years away given the dimensionality of the problem and the complex structure of singularities above breakup. For elastic and transfer reactions driven by all possible N+3N

initial states as well as d+d, converged solutions for all two-body reactions up to 30 MeV beam energy [8–10] are available. Going to higher energies is formally not an obstacle but requires much more computer power to obtain fully converged results in terms of number of partial waves and grid points. On the other hand, the existing d+d breakup measurement [11–13] performed at 130 MeV deuteron beam energy has provided fully exclusive cross sections that are about three orders of magnitude smaller than for the p+d breakup at comparable energies. This is puzzling because one would expect a similar order of magnitude for p+d and d+d total breakup cross sections. According to recent calculations, albeit at the much lower energy of 10 MeV [9], this is indeed the case.

Therefore, in order to provide the first estimate of d+d breakup cross sections at higher energies, we present here an approximate calculation based on the lowest-order term in the Neumann series expansion of the Alt, Grassberger and Sandhas (AGS) equations [14] for the breakup operator and called single-scattering approximation (SSA). The SSA contains the breakup of one of the deuterons followed by the scattering of one nucleon from the other deuteron through the full 3N operator that sums up all orders of NN rescattering involving the corresponding three particles. This operator is obtained from the exact solution of the AGS three-nucleon equations for the underlying force model being used. As demonstrated before [15], the same kind of approximation may be used to calculate d+d elastic scattering at high energies. In order to obtain a quantitative calibration of the d+d breakup cross sections, we provide SSA results also for d+d elastic scattering observables.

SSA for three-cluster breakup calculations is expected

to be reasonable near quasi-free scattering (QFS) kinematics at energies above 100 MeV in the center-of-mass (c.m.) system. This conjecture is supported by the results for the equivalent approximation applied to p+d breakup where a comparison with the exact results that include NN rescattering to all orders is possible.

In Section II we present the theory for the breakup amplitudes using the first term in the Neumann series expansion of the AGS equations, and study the equivalent approximation applied to p+d breakup by comparing such results with those obtained from the exact solution of the corresponding 3N problem. In Section III we show the results for d+d elastic scattering and three-cluster breakup near the quasi-free scattering kinematics. Conclusions come in Section IV.

II. SCATTERING AMPLITUDES

We start with exact four-nucleon scattering equations and transition amplitudes, and then show how they are simplified under the single scattering approximation. Treating nucleons as identical fermions in the isospin formalism, one has to consider only two two-cluster partitions, namely, 3 + 1 and 2 + 2 which in the notation for operators and wave-functions are abbreviated by 1 and 2, respectively. In terms of four particles 1,2,3, and 4 they correspond to the clustering (12,3)4 and (12)(34), respectively. The reactions initiated by the collisions of two deuterons are described by the four-nucleon transition operators $\mathcal{U}_{\beta 2}$ obeying the symmetrized AGS equations

$$\mathcal{U}_{12} = (G_0 t G_0)^{-1} - P_{34} U_1 G_0 t G_0 \mathcal{U}_{12} + U_2 G_0 t G_0 \mathcal{U}_{22}, \quad (1a)$$

$$\mathcal{U}_{22} = (1 - P_{34}) U_1 G_0 t G_0 \mathcal{U}_{12}. \quad (1b)$$

The pair potential v enters the AGS equations via the pair (12) transition matrix

$$t = v + v G_0 t \quad (2)$$

and via the 3+1 and 2+2 subsystem transition operators

$$U_\alpha = P_\alpha G_0^{-1} + P_\alpha t G_0 U_\alpha. \quad (3)$$

The dependence of all transition operators on the available energy E , although not indicated in our notation, arises via the free resolvent

$$G_0 = (E + i0 - H_0)^{-1} \quad (4)$$

where H_0 is the free Hamiltonian. In the considered case $E = p_2^2/2m_N + 2\epsilon_d$, where p_2 is the relative d - d momentum, m_N the average nucleon mass, and $\epsilon_d = -2.225$ MeV the energy of the deuteron bound state. The full antisymmetry that a system of four identical fermions must obey is ensured by the permutation operators P_{ab} of nucleons a and b with $P_1 = P_{12} P_{23} + P_{13} P_{23}$ and

$P_2 = P_{13} P_{24}$. Furthermore, the basis states are antisymmetric under exchange of the two nucleons (12) while in the 2 + 2 partition they are antisymmetric also under exchange of the two nucleons (34).

The three-cluster breakup operator for the 2 + 2 collision is derived in Ref. [16] to be

$$\mathcal{U}_{32} = (1 - P_{34}) U_1 G_0 t G_0 \mathcal{U}_{12} + U_2 G_0 t G_0 \mathcal{U}_{22}. \quad (5)$$

To get the reaction amplitudes the on-shell matrix elements of the above transition operators have to be calculated between the appropriate channel states. Considering only the elastic d - d scattering and three-cluster breakup, the respective channel states are $|\Phi_2(\mathbf{p}_2)\rangle = |\phi_d \phi_d \mathbf{p}_2\rangle = (1 + P_2) |\phi_2(\mathbf{p}_2)\rangle$ with the Faddeev component $|\phi_2(\mathbf{p}_2)\rangle = G_0 v |\Phi_2(\mathbf{p}_2)\rangle = G_0 t P_2 |\phi_2(\mathbf{p}_2)\rangle$, and $|\Phi_3(\mathbf{k}_y, \mathbf{k}_z)\rangle = |\phi_d \mathbf{k}_y \mathbf{k}_z\rangle$. Here ϕ_d denotes the deuteron wave function, \mathbf{p}_2 is the relative d - d momentum, and \mathbf{k}_y and \mathbf{k}_z are momenta for the relative motion in the three-cluster $d + p + n$ system, e.g., $\mathbf{k}_y = (2\mathbf{k}_p - \mathbf{k}_d)/3$ and $\mathbf{k}_z = (3\mathbf{k}_n - \mathbf{k}_p - \mathbf{k}_d)/4$ for the $(dp)n$ partition. The dependence on the discrete spin and isospin quantum numbers is suppressed in our notation. The elastic and three-cluster breakup amplitudes are

$$\langle \mathbf{p}'_2 | \mathcal{T}_{22} | \mathbf{p}_2 \rangle = 2 \langle \phi_2(\mathbf{p}'_2) | \mathcal{U}_{22} | \phi_2(\mathbf{p}_2) \rangle, \quad (6a)$$

$$\langle \mathbf{k}_y \mathbf{k}_z | \mathcal{T}_{32} | \mathbf{p}_2 \rangle = 2 \langle \Phi_3(\mathbf{k}_y, \mathbf{k}_z) | \mathcal{U}_{32} | \phi_2(\mathbf{p}_2) \rangle. \quad (6b)$$

Factors of 2 result from the antisymmetrization of the four-nucleon states [16]; to account for the identity of the two deuterons one has to use symmetrized d - d channel states, leading to symmetrized amplitudes obtained from (6) by replacing $|\phi_2(\mathbf{p}_2)\rangle$ with $|\phi_2^s(\mathbf{p}_2)\rangle = \frac{1}{\sqrt{2}}(1 + P_2) |\phi_2(\mathbf{p}_2)\rangle = \frac{1}{\sqrt{2}}[|\phi_2(\mathbf{p}_2)\rangle + |\phi_2^x(-\mathbf{p}_2)\rangle]$ where the superscript x indicates that also the spin-isospin part is exchanged. Note that in the partial-wave representation both terms have equal contributions.

The absence of an inhomogeneous term in the equation (1b) makes possible the development of a simple approximation for d+d elastic scattering and three-cluster breakup that may work at higher energies under certain conditions. In the single-scattering approximation only the terms that are of first order in the subsystem transition operators U_α are retained, resulting in the amplitudes

$$\langle \mathbf{p}'_2 | \mathcal{T}_{22}^{\text{SS}} | \mathbf{p}_2 \rangle = 2 \langle \phi_2^s(\mathbf{p}'_2) | (1 - P_{34}) U_1 | \phi_2^s(\mathbf{p}_2) \rangle, \quad (7a)$$

$$\langle \mathbf{k}_y \mathbf{k}_z | \mathcal{T}_{32}^{\text{SS}} | \mathbf{p}_2 \rangle = 2 \langle \Phi_3(\mathbf{k}_y, \mathbf{k}_z) | (1 - P_{34}) U_1 | \phi_2^s(\mathbf{p}_2) \rangle. \quad (7b)$$

Thus, only the calculation of the operator U_1 is required, which is the standard three-nucleon AGS transition matrix. However, it needs to be calculated at off-shell momenta as we show below. Given that $|\phi_2(\mathbf{p}_2)\rangle = G_0 v |\phi_d \phi_d \mathbf{p}_2\rangle$, it is convenient to introduce the momentum-space matrix elements

$$\langle \phi_d \mathbf{k}_y \mathbf{k}_z | v G_0 U_1 G_0 v | \phi_d \mathbf{k}'_y \mathbf{k}'_z \rangle = \delta(\mathbf{k}_z - \mathbf{k}'_z) \bar{U}_1(\mathbf{k}_y, \mathbf{k}'_y, k_z) \quad (8)$$

and the deuteron wave function $\phi_d(\mathbf{p}_y) = \langle \mathbf{p}_y | \phi_d \rangle$; they are operators in the spin-isospin space. With these definitions the first contribution to the symmetrized SSA elastic amplitude (7) is calculated as

$$\begin{aligned} & \langle \phi_2(\mathbf{p}'_2) | (1 - P_{34}) U_1 | \phi_2(\mathbf{p}_2) \rangle \\ & = 2 \int d^3 \mathbf{k}_z \phi_d(\mathbf{p}'_y) \bar{U}_1(\mathbf{k}_y, \mathbf{k}'_y, k_z) \phi_d(\mathbf{p}_y) \end{aligned} \quad (9)$$

with

$$\mathbf{p}'_y = \frac{1}{2} \mathbf{p}'_2 - \mathbf{k}_z, \quad (10a)$$

$$\mathbf{p}_y = \frac{1}{2} \mathbf{p}_2 - \mathbf{k}_z, \quad (10b)$$

$$\mathbf{k}'_y = \mathbf{p}_2 - \frac{2}{3} \mathbf{k}_z, \quad (10c)$$

$$\mathbf{k}_y = \mathbf{p}'_2 - \frac{2}{3} \mathbf{k}_z. \quad (10d)$$

The remaining three contributions are calculated analogously. In Eq. (9) the energy available for the three-nucleon subsystem $E - 2k_z^2/3m_N$ runs from E to $-\infty$, obviously indicating that U_1 is needed off-shell. On the other hand, the final breakup channel state $|\Phi_3(\mathbf{k}_y, \mathbf{k}_z)\rangle$ fulfills the on-shell condition $E = \epsilon_d + 3k_y^2/4m_N + 2k_z^2/3m_N$, indicating that only half-shell elements of U_1 are needed. Thus, the first term of the single-scattering breakup amplitude (7b) becomes

$$\langle \Phi_3(\mathbf{k}_y, \mathbf{k}_z) | U_1 | \phi_2(\mathbf{p}_2) \rangle = \bar{U}_1(\mathbf{k}_y, \mathbf{k}'_y, k_z) \phi_d(\mathbf{p}_y) \quad (11)$$

with \mathbf{k}'_y and \mathbf{p}_y defined in Eqs. (10). The second term is calculated analogously, but with the final state $P_{34}|\Phi_3(\mathbf{k}_y, \mathbf{k}_z)\rangle = |\Phi_3^x(\frac{1}{3}\mathbf{k}_y + \frac{8}{9}\mathbf{k}_z, \mathbf{k}_y - \frac{1}{3}\mathbf{k}_z)\rangle$ where the superscript x indicates that also the spin-isospin part is exchanged. These two contributions are graphically depicted in Fig. 1 for the $d+p+n$ final state. Taking the left-side deuteron as the beam and the right-side deuteron as the target, the diagram (a) corresponds to the target deuteron breakup after the full interaction between the impinging deuteron and the target proton while no interaction occurs involving the target neutron. Thus, the diagram (a) corresponds to proton-deuteron quasi-free scattering (QFS). Analogously, the diagram (b) corresponds to neutron-deuteron QFS. Two more contributions $\langle \Phi_3(\mathbf{k}_y, \mathbf{k}_z) | (1 - P_{34}) U_1 | \phi_2^x(-\mathbf{p}_2) \rangle$, not shown in Fig. 1, arise due to the symmetrization of the initial $d+d$ state; they correspond to the breakup of the impinging deuteron.

Under the assumption of the simplified SSA reaction mechanism of Fig. 1 (a), the energy distribution of the final neutron is given by the deuteron wave function, i.e., the differential cross section is sharply peaked at the neutron energy $E_n = 0$. In a complete reaction picture the cross section also gets contributions from the higher rescattering terms beyond the SSA; roughly, their relative importance increases when the SSA contribution decreases, i.e., for larger E_n . Thus, the reliability of

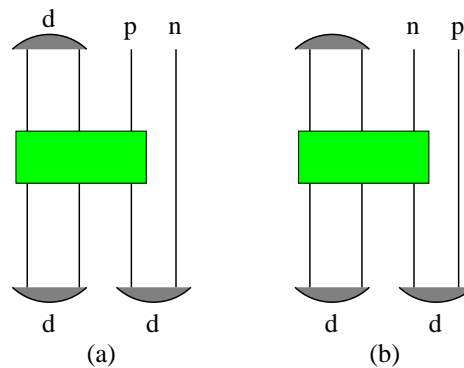


FIG. 1. (Color online) Two contributions to the single-scattering three-cluster breakup amplitude. The three-nucleon transition operator U_1 is represented by a box while deuterons are represented by filled arcs.

the SSA should decrease with increasing energy of the final neutron. Another necessary condition for the non-interacting neutron, and thereby also for the validity of the SSA, is a high enough relative $n-d$ and $n-p$ energy, implying also high enough energy for the initial beam and for the final deuteron and proton. At $E_n = 0$ only the contribution of Fig. 1 (a) is peaked; the remaining three SSA contributions are not as they do not correspond to the deuteron-proton(target) QFS. In the following we will call the results obtained with only the contribution of Fig. 1 (a) as SSA-1, while those including all four contributions as SSA-4. An agreement between the SSA-1 and SSA-4 results indicates the dominance of the Fig. 1 (a) SSA reaction mechanism, while disagreement indicates a more complicated reaction mechanism; a significant contribution of higher-order terms is probable in the latter case although it cannot be ruled out also in the former case.

Finally we note that the corresponding SSA can be introduced also in the nucleon-deuteron scattering, expanding the three-nucleon transition operators in terms of two-nucleon transition operators t and retaining first order terms in the Neumann series. In fact, this approach already has been used in a number of early works, e.g. [17]. The full nucleon-deuteron breakup operator is

$$U_0 = (1 + P_1)t G_0 U_1 \quad (12)$$

whereas its SSA reads

$$U_0^{\text{SS}} = (1 + P_1)t P_1. \quad (13)$$

The diagrammatic representation of the nucleon-deuteron SSA is very similar to the one of Fig. 1 except that the left-side deuteron is replaced by a nucleon and the three-nucleon transition operator U_1 is replaced by the two-nucleon operator t .

Comparing results based on Eqs. (12) and (13) one can evaluate the reliability of the SSA in three-nucleon

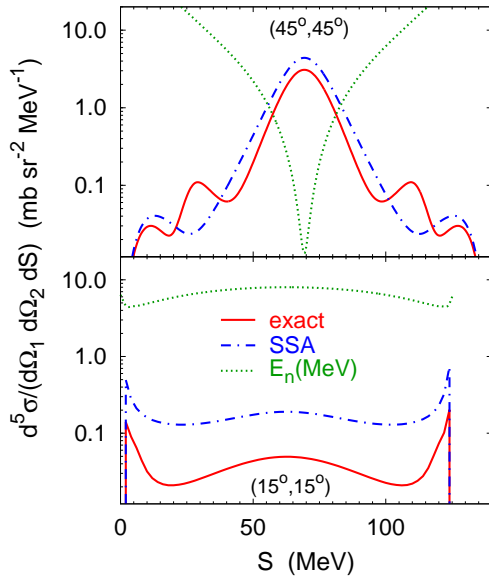


FIG. 2. (Color online) Differential cross section for the proton deuteron breakup at 95 MeV proton beam energy as function of the arclength S along the kinematical curve. The polar angles of the two detected protons (θ_1, θ_2) are indicated in the plots. Exact results based on the CD Bonn + Δ potential and including the Coulomb interaction (solid curves) are compared with SSA results (dashed-dotted curves) that neglect the Coulomb interaction. The final neutron energy is given by dotted curves.

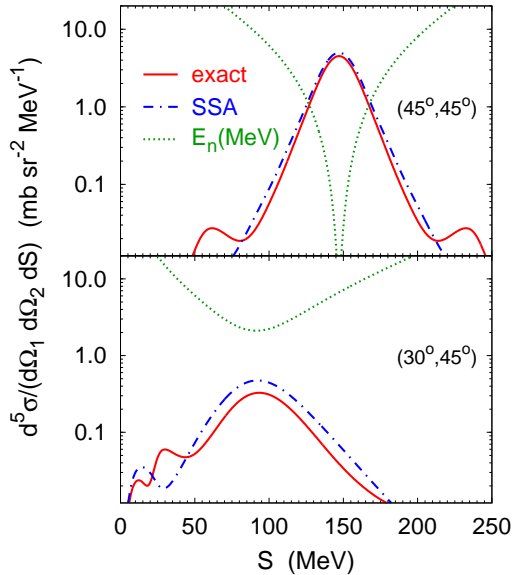


FIG. 3. (Color online) Same as Fig. 2 but at 200 MeV proton beam energy.

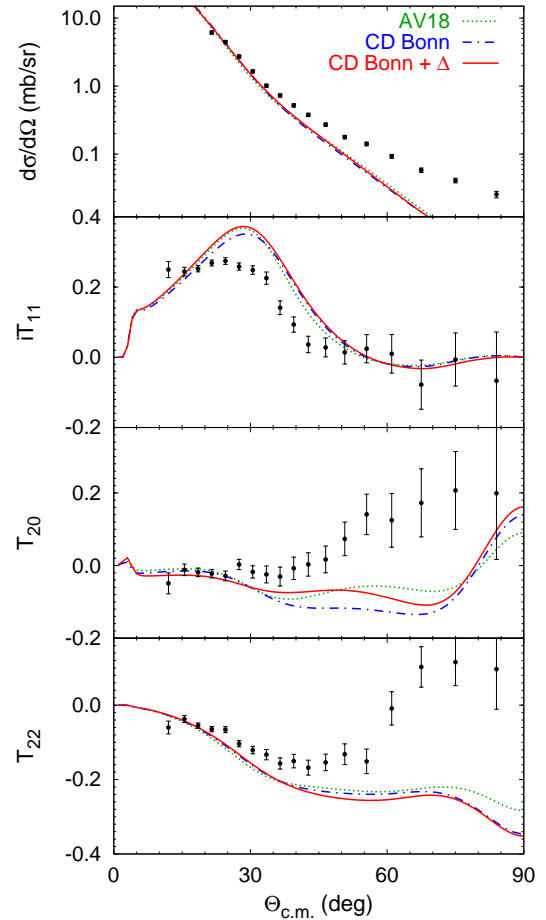


FIG. 4. (Color online) Differential cross section and deuteron analyzing powers for the deuteron-deuteron elastic scattering at 232 MeV deuteron beam energy. SSA predictions based on the CD Bonn + Δ (solid curves), CD Bonn (dashed-dotted curves), and AV18 (dotted curves) potentials are compared with experimental data from Ref. [15].

breakup. This is done in Figs. 2 and 3 for proton-deuteron breakup at 95 and 200 MeV proton beam energy in several kinematical configurations. The above energy values approximately correspond to the same c.m. energy as 130 and 270 MeV deuteron energy in deuteron-deuteron collisions. The fivefold differential cross section $d^5\sigma/d\Omega_1 d\Omega_2 dS$ is shown as a function of the arclength S along the kinematical curve for fixed angles of the two detected protons ($\theta_1, \varphi_1 = 0^\circ$) and ($\theta_2, \varphi_2 = 180^\circ$). The energy of the neutron E_n is plotted as well. One can see that the SSA results deviate significantly from the exact ones for larger E_n values; for small E_n well below 1 MeV the agreement improves for higher proton beam energy.

Total p+d breakup cross sections calculated exactly and in the SSA are 69.1 and 109 mb at 95 MeV and 49.7 and 63.5 mb at 200 MeV, respectively. Thus, SSA provides a correct order of the magnitude for the p+d total breakup cross section.

III. RESULTS

We use three models of realistic high-precision two-nucleon potentials, namely, the Argonne 18-operator (AV18) potential [18], the charge-dependent Bonn potential (CD Bonn) [19], and its extension CD Bonn + Δ [20] allowing for an excitation of a nucleon to a Δ isobar and thereby yielding an effective 3N force.

The three-nucleon AGS equation (3) is solved in the momentum-space partial-wave representation. The states with two-nucleon angular momenta $j_x \leq 5$ and three-nucleon angular momenta $j_y \leq \frac{27}{2}$ are included. The final four-nucleon results are well converged with these cutoffs. The elastic amplitude (7a) is calculated in partial waves including the states with 4N total angular momentum $J \leq 25$ while for the breakup amplitude the obtained partial-wave half-shell matrix elements of U_1 are first transformed into the plane-wave basis and then used in Eq. (7b). The Coulomb interaction is neglected when solving AGS equation (3) for the 3N transition operator U_1 . However, the external Coulomb correction is added to the elastic amplitude (7a).

We first present results for d+d elastic observables at 232 MeV beam energy where the experimental data [15] for the differential cross section and analyzing powers are available. The SSA results based on Eq. (7a) are shown in Fig. 4 for CD Bonn + Δ , CD Bonn and AV18 potentials. The sensitivity to the force model is visible for the tensor analyzing powers T_{20} and T_{22} . The observables are reasonably described at forward scattering angles $\Theta_{\text{c.m.}} \leq 40^\circ$ in the c.m. frame. At larger scattering angles multiple scattering effects are expected, thus, the failure of SSA is not surprising. For the vector analyzing power iT_{11} a rough agreement between SSA results and experimental data is seen also at larger angles. Since the calculation of the d+d elastic amplitude involves the integration of the N+d off-shell amplitude over the 3N subsystem energy range from E to $-\infty$, it is reasonable to assume that the SSA for the d+d breakup may have the correct order of magnitude over a wide range of phase space. Therefore we expect our SSA results to provide at least the correct order of magnitude for the d+d three-cluster breakup cross sections.

The fivefold differential cross section for the three-cluster breakup in the laboratory frame

$$\begin{aligned} \frac{d^5\sigma}{d\Omega_d d\Omega_p dS} &= (2\pi)^4 \frac{m_N}{p_2} |\langle \mathbf{k}_y \mathbf{k}_z | \mathcal{T}_{32}^{\text{SS}} | \mathbf{p}_2 \rangle|^2 m_N^2 k_d^2 k_p^2 \\ &\times \left\{ (k_d/2)^2 [2k_p - \hat{\mathbf{k}}_p \cdot (2\mathbf{p}_2 - \mathbf{k}_d)]^2 \right. \\ &\left. + k_p^2 [3k_d/2 - \hat{\mathbf{k}}_d \cdot (2\mathbf{p}_2 - \mathbf{k}_p)]^2 \right\}^{-1/2}. \end{aligned} \quad (14)$$

is calculated as a function of the arclength S along the kinematical curve in the plane of final deuteron and proton energies E_d and E_p for fixed polar and azimuthal angles of the deuteron ($\theta_d, \varphi_d = 0^\circ$) and proton ($\theta_p, \varphi_d =$

180°). The starting point $S = 0$ is chosen as $E_p = 0$ with $dE_p/dE_d > 0$ and S is measured counterclockwise in the (E_d, E_p) plane.

The spin-averaged differential cross section for six angular configurations is shown in Fig. 5, together with the energy E_n of the final-state neutron; the CD Bonn + Δ model is used. This observable is peaked at the minimum of E_n , i.e., near/at deuteron-proton QFS kinematics. The SSA-1 and SSA-4 predictions approach each other for small E_n and deviate at larger E_n . The experimental data [11] taken at KVI are preliminary and cannot be shown here except for the configuration $(\theta_d, \theta_p) = (15^\circ, 15^\circ)$ already published in Ref. [12]. The disagreement between our predictions and data exceeds a factor of 1000 which is striking. In fact, when compared to the data [11], a similar discrepancy of three orders of magnitude exists for all remaining configurations in Fig. 5. Such a difference is far too large even taking into account that our predictions are approximate. On the other hand, using SSA we predict the same order of magnitude for the differential cross section in nucleon-deuteron and deuteron-deuteron three-cluster breakup. This applies also to the total three-cluster breakup cross section. Using SSA-4 with the CD Bonn + Δ potential we obtain 189 and 57 mb at 130 and 270 MeV, respectively, which are comparable to the ones in nucleon-deuteron breakup. Since in the nucleon-deuteron breakup the SSA provides the right order of magnitude for both differential and total cross sections, we believe that our predictions for the deuteron-deuteron three-cluster breakup are reasonable as well and point out to problems in the experimental data of Ref. [11]. These conclusions are supported by very recent measurements of this reaction at 160 MeV deuteron beam energy where our differential cross section predictions near QFS kinematics are in qualitative agreement with the preliminary experimental data [21].

Deuteron vector analyzing power iT_{11} and tensor analyzing powers T_{20} and T_{22} are shown in Figs. 6 — 8 for several kinematic (θ_d, θ_p) configurations. The experimental data points for two of them, $(15^\circ, 15^\circ)$ and $(25^\circ, 25^\circ)$, are taken from Ref. [13], others are still preliminary and only available in Ref. [11]. There is a rough qualitative agreement between the data and SSA-1 and SSA-4 predictions for $(15^\circ, 15^\circ)$ and $(25^\circ, 20^\circ)$ configurations. The data change very rapidly from $(25^\circ, 20^\circ)$ to $(25^\circ, 25^\circ)$, losing the agreement with SSA results. Comparing SSA-1 and SSA-4 predictions one may conclude that the level of agreement between SSA-1 and SSA-4 is not the same for the spin-averaged differential cross section and for spin observables. The sensitivity of all these observables to the force model is minor and it is not shown.

Although no experimental data is available above 160 MeV, we present in Fig. 9 example results at 270 MeV deuteron beam energy where the sensitivity to the force model becomes more visible. Under suitable kinematic conditions, e.g., in the $(28^\circ, 25^\circ)$ configuration, this sensitivity even exceeds the difference between SSA-1 and SSA-4. Nevertheless it is plausible that this extra sen-

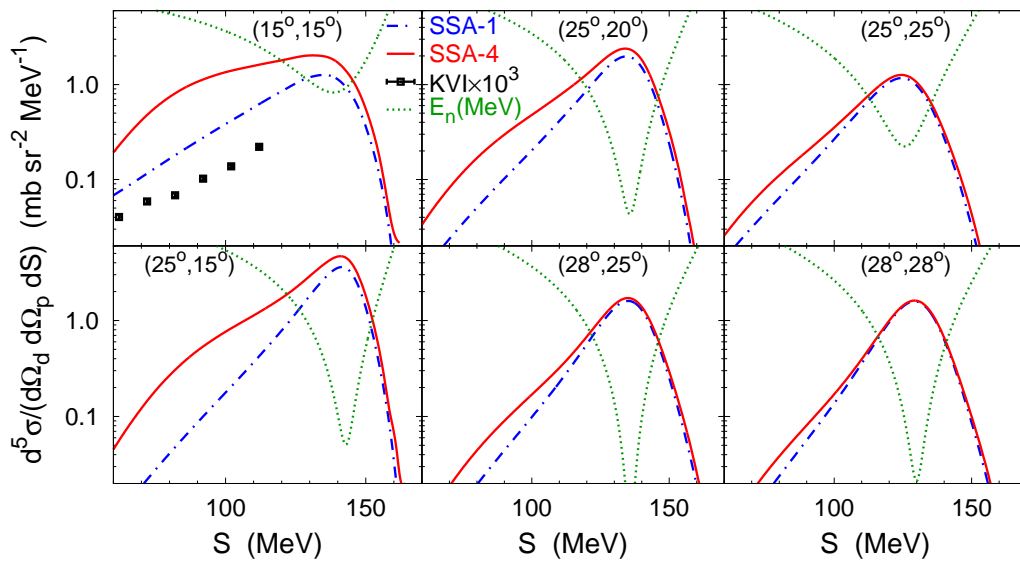


FIG. 5. (Color online) Differential cross section for the three-cluster breakup in deuteron-deuteron collision at 130 MeV deuteron beam energy as function of the arclength S along the kinematical curve. The polar angles of the detected deuteron and proton (θ_d, θ_p) are indicated in the plots, the azimuthal angles are $(\varphi_d, \varphi_p) = (0^\circ, 180^\circ)$. SSA 4-term (solid curves) and 1-term (dashed-dotted curves) results, both based on the CD Bonn + Δ potential, are compared. Published experimental data from Ref. [12] are only available for the configuration $(15^\circ, 15^\circ)$; in the plot the data points are multiplied by a factor of 10^3 . The final neutron energy is given by dotted curves.

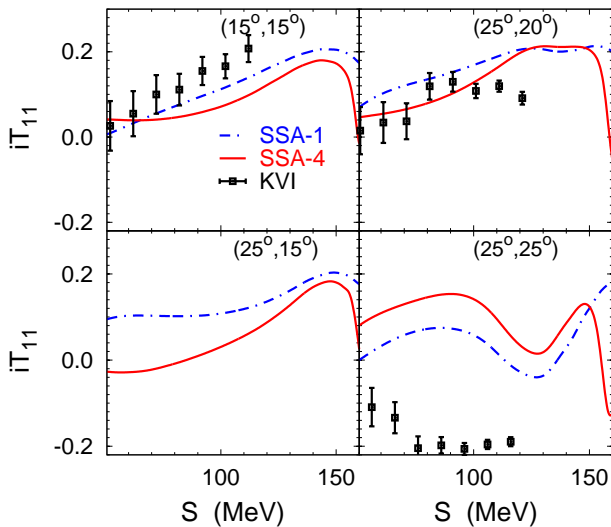


FIG. 6. (Color online) Deuteron analyzing power iT_{11} for the three-cluster breakup in deuteron-deuteron collision at 130 MeV deuteron beam energy. The polar angles of the detected deuteron and proton (θ_d, θ_p) are indicated in the plots. SSA 4-term (solid curves) and 1-term (dashed-dotted curves) results, both based on the CD Bonn + Δ potential, are compared with the experimental data from Refs. [11, 13].

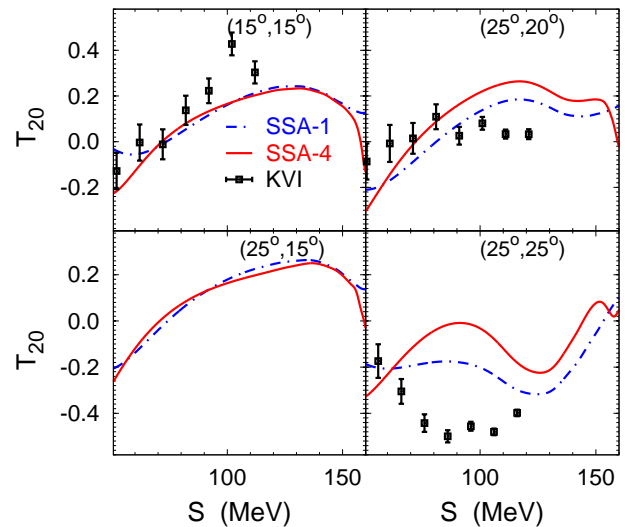


FIG. 7. (Color online) Deuteron tensor analyzing power T_{20} for the three-cluster breakup in deuteron-deuteron collision at 130 MeV deuteron beam energy. Curves and experimental data are as in Fig. 6.

IV. SUMMARY

In the present work we have calculated the spin-averaged fivefold differential cross section and deuteron analyzing powers for the three-cluster breakup in deuteron-deuteron collisions at 130 and 270 MeV beam

sensitivity may change when exact calculations are performed.

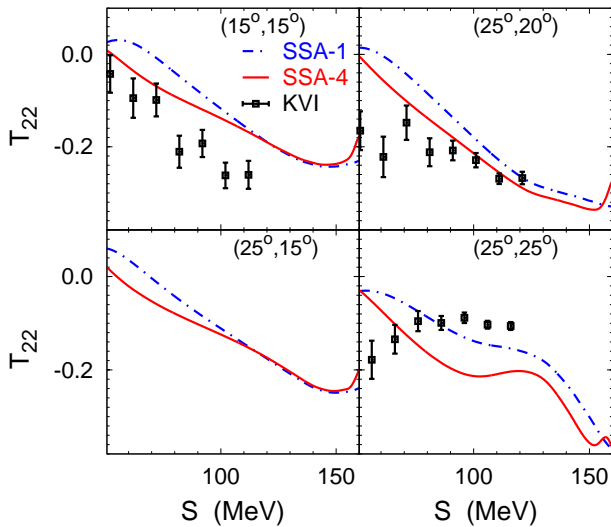


FIG. 8. (Color online) Deuteron tensor analyzing power T_{22} for the three-cluster breakup in deuteron-deuteron collision at 130 MeV deuteron beam energy. Curves and experimental data are as in Fig. 6.

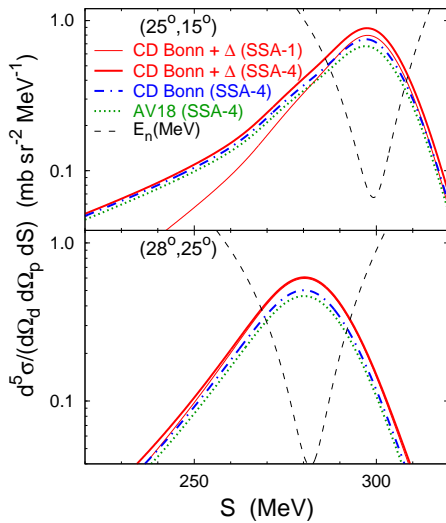


FIG. 9. (Color online) Differential cross section for the three-cluster breakup in deuteron-deuteron collision at 270 MeV deuteron beam energy. The polar angles of the detected deuteron and proton (θ_d, θ_p) are indicated in the plots. SSA-4 based on the CD Bonn + Δ (solid curves), CD Bonn (dashed-dotted curves), and AV18 (dotted curves) potentials are compared with the SSA-1 predictions based on the CD Bonn + Δ potential (thin solid curves). The final neutron energy is given by dashed curves.

energy. Although at this time we could not perform an exact four-nucleon calculation of the corresponding breakup amplitudes, we devised an approximation based on the first term in the Neumann series expansion of the AGS three-cluster breakup operator which is expected to be, qualitatively, a reasonable approximation near proton-deuteron quasifree scattering kinematic conditions.

In order to validate the method, we calculated proton-deuteron breakup at similar energies and compared with the results of an exact three-nucleon calculation. Likewise we used the same single scattering approximation to calculate deuteron-deuteron elastic scattering at 232 MeV where there is data for the differential cross section and analyzing powers. These auxiliary studies have shown that the SSA reproduces, if nothing else, the correct magnitude of the existing cross section data.

Although the deuteron beam energy of 130 MeV seems to be not high enough for SSA to be reliable, we compared the SSA results for the three-cluster breakup with the experimental data measured at KVI [11–13]. We found, at least in some configurations, a rough qualitative agreement for deuteron analyzing powers, but a factor of 1000 difference for the cross section. Since we have provided convincing arguments that SSA should yield at least correct order of magnitude for total and differential cross sections, and that deuteron-deuteron and proton-deuteron breakup cross sections should be of comparable size, our work raises some serious concern on the correct normalization of the KVI data. On the contrary, new Cracow data [21] at 160 MeV seems to be in line with our SSA results. Further investigation on these issues needs to be pursued by both theory and experimental collaborations.

We thank A. Ramazani-Moghaddam-Arani and N. Kalantar-Nayestanaki for discussions and providing the experimental data.

[1] A. Kievsky, M. Viviani, and S. Rosati, Phys. Rev. C **64**, 024002 (2001).
 [2] J. Strate *et al.*, Nucl. Phys. **A501**, 51 (1989).

[3] H. R. Setze *et al.*, Phys. Rev. C **71**, 034006 (2005).
 [4] A. Deltuva, A. C. Fonseca, and P. U. Sauer, Phys. Rev. C **72**, 054004 (2005).

- [5] A. Deltuva and A. C. Fonseca, Phys. Rev. C **76**, 021001(R) (2007).
- [6] R. Lazauskas, Phys. Rev. C **79**, 054007 (2009).
- [7] M. Viviani, L. Girlanda, A. Kievsky, and L. E. Marcucci, Phys. Rev. Lett. **111**, 172302 (2013).
- [8] A. Deltuva and A. C. Fonseca, Phys. Rev. Lett. **113**, 102502 (2014).
- [9] A. Deltuva and A. Fonseca, Phys. Lett. B **742**, 285 (2015).
- [10] R. Lazauskas, Phys. Rev. C **91**, 041001 (2015).
- [11] A. Ramazani-Moghaddam-Arani, Ph.D. thesis, University of Groningen, 2009.
- [12] A. Ramazani-Moghaddam-Arani *et al.*, EPJ Web of Conferences **3**, 04012 (2010).
- [13] A. Ramazani-Moghaddam-Arani *et al.*, Phys. Rev. C **83**, 024002 (2011).
- [14] P. Grassberger and W. Sandhas, Nucl. Phys. **B2**, 181 (1967); E. O. Alt, P. Grassberger, and W. Sandhas, JINR report No. E4-6688 (1972).
- [15] A. M. Micherdzinska *et al.*, Phys. Rev. C **75**, 054001 (2007).
- [16] A. Deltuva, Few-Body Syst. **54**, 2419 (2013).
- [17] S. Fukehara, T. Okino, A. Shibata, and T. Takemiya, Prog. Theor. Phys. **62**, 107 (1979).
- [18] R. B. Wiringa, V. G. J. Stoks, and R. Schiavilla, Phys. Rev. C **51**, 38 (1995).
- [19] R. Machleidt, Phys. Rev. C **63**, 024001 (2001).
- [20] A. Deltuva, R. Machleidt, and P. U. Sauer, Phys. Rev. C **68**, 024005 (2003).
- [21] G. Khatri, Ph.D. thesis, Jagiellonian University, Cracow, 2015.